JACS
JOURNAL OF THE AMERICAN CHEMICAL SOCIETY

Communication

pubs.acs.org/JACS

# Porphyrin Shell Microbubbles with Intrinsic Ultrasound and Photoacoustic Properties

Elizabeth Huynh,[†,‡] Jonathan F. Lovell,[†,§,⊥] Brandon L. Helfield,[‡,∥] Mansik Jeon,[⊥] Chulhong Kim,[⊥] David E. Goertz,[‡,∥] Brian C. Wilson,[†,‡] and Gang Zheng*[,†,‡,§]

[†]Ontario Cancer Institute and Techna Institute, University Health Network, Toronto, Ontario, Canada M5G 1L7

[‡]Department of Medical Biophysics, University of Toronto, Toronto, Ontario, Canada M5G 1L7

[§]Institute of Biomaterials and Biomedical Engineering, University of Toronto, Toronto, Ontario, Canada M5G 1L7

[∥]Sunnybrook Health Sciences Center, University of Toronto, Toronto, Ontario, Canada M4N 3M5

[⊥]Department of Biomedical Engineering, University at Buffalo, State University of New York, Buffalo, New York 14260, United States

Supporting Information

**ABSTRACT:** Porphyrin−phospholipid conjugates were used to create photonic microbubbles (MBs) having a porphyrin shell ("porshe"), and their acoustic and photoacoustic properties were investigated. The inclusion of porphyrin−lipid in the MB shell increased the yield, improved the serum stability, and generated a narrow volumetric size distribution with a peak size of 2.7 ± 0.2 $\mu$m. Using an acoustic model, we calculated the porshe stiffness to be 3−5 times greater than that of commercial lipid MBs. Porshe MBs were found to be intrinsically suitable for both ultrasound and photoacoustic imaging with a resonance frequency of 9−10 MHz. The distinctive properties of porshe MBs make them potentially advantageous for a broad range of biomedical imaging and therapeutic applications.

Ultrasound (US) is a widely used imaging modality in clinical practice. Microbubble (MB) contrast agents enhance acoustic differentiation between blood vessels and surrounding tissue as a result of their highly scattering acoustic properties and nonlinear responses to incident US. Commercially available US MBs, which are typically 1−10 $\mu$m in diameter, are composed of fluorinated gases encapsulated within a biocompatible shell composed of lipids, albumin, or polymers. The shell minimizes the surface tension at the gas−liquid interface, while the fluorinated gases have low solubility in blood. Both components stabilize the gas core and prolong the lifetime.[1] MBs are routinely used in the clinic for low-frequency applications ($f$ < 5 MHz) to observe blood flow in the heart, liver, and kidneys[2] for diagnosis and treatment guidance of focal lesions.[3] More recently, MB applications exploiting conventional diagnostic imaging platforms with higher-frequency transducers ($f$ = 5−15 MHz) are beginning to gain interest, including breast imaging[4] and carotid neovascularization detection.[5] In addition, the use of MBs for molecular imaging,[6] US-triggered drug and gene delivery,[7] and vasculature remodeling[8] have been investigated preclinically for various diseases. In these preclinical studies, fluorescent molecules are often incorporated into the MB shell to verify targeting[9] and/or US-mediated MB disruption.[10] However, the influence of these fluorophore molecules on the properties of MBs has not been widely investigated, and the fluorophore fraction within the shell is normally very small.

Photoacoustic tomography (PAT) is an emerging technology that provides high-resolution imaging and significantly greater penetration depth than other optical imaging modalities. It is based on the local absorption of short (∼ns) pulsed laser light in tissue, resulting in transient thermoelastic expansion and the generation of pressure waves that are then detected by a conventional US transducer. PAT can provide functional and metabolic information using endogenous optical absorbers such as melanin and hemoglobin in addition to molecular and genetic imaging with the use of exogenous contrast agents.[11] There has been a recent growing interest in combined US/PA imaging to produce simultaneous morphological and physiological information through the mechanical contrast generated from US and the optical contrast from PAT.[12]

Despite the complementary information provided by this dual-modality approach, limitations on US contrast and interference by endogenous optical absorbers in PAT persist without the use of a contrast agent. Only a few dual-modality US/PA contrast agents have been proposed, many of which involve complicated encapsulation or tethering of the optical absorber to an US-compatible micro- or nanobubble.[13] Here we report the first intrinsically dual-modality US/PA agent with one-step synthesis, through the formation of a MB shell with porphyrin−lipid conjugates.

We previously introduced a new paradigm for the formation of phospholipid bilayer nanovesicles entirely from porphyrin−lipid conjugates having structure-dependent photonic properties.[14] Here we describe MBs formed from a porphyrin−lipid shell encapsulating a fluorinated gas, termed "porshe microbubbles" (Figure 1a). These were synthesized using a mechanical agitation method as follows. Lipid films containing the porphyrin−lipid 1-stearoyl-2-pyropheophorbide-*sn*-glycero-3-phosphocholine and the phospholipid 1,2-distearoyl-*sn*-glycero-3-phosphocholine (DSPC) were rehydrated with a solution of polyoxyethylene-40 stearate (PEG40S) and phosphate-buffered saline (PBS), and the headspace of the vial was filled with one of various fluorinated gases. After dispersion of the lipid film, MBs were formed using a

**Received:** June 19, 2012
**Published:** July 24, 2012





dx.doi.org/10.1021/ja305988f | *J. Am. Chem. Soc.* 2012, 134, 16464−16467

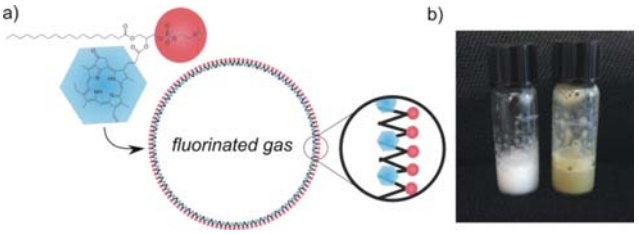


**Figure 1.** (a) Schematic of porshe microbubbles (MBs) formed from a monolayer of porphyrin−lipid mixed with regular phospholipid encapsulating a fluorinated gas. (b) Image of MBs formed (right) with and (left) without 15 mol % porphyrin−lipid.

Vialmix activator (Lantheus Medical Imaging), the device used for activation of commercial Definity MBs (Lantheus Medical Imaging). The activator produces high-shear gas dispersion in the aqueous solution, affording lipid-encapsulated MBs.[15]

To investigate the effects of the porphyrin−lipid on the MB shell, increasing molar concentrations of porphyrin−lipid were titrated into a MB formulation. Unexpectedly, with 5−20 mol % porphyrin−lipid incorporation, the MBs were formed in significantly higher yield than without porphyrin−lipid for a variety of fluorinated gases (Figure 2a). We hypothesize that the

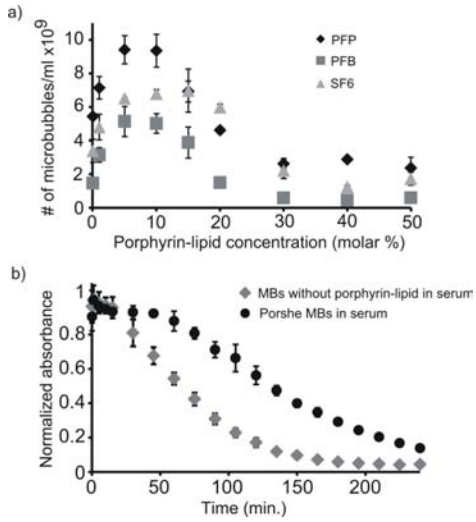


**Figure 2.** Porshe MB yield and serum stability. (a) Number of MBs ($\times 10^9$) per mL as a function of the amount of porphyrin−lipid included in a control formulation for different filling gases: perfluoropropane (PFP), perfluorobutane (PFB), and sulfur hexafluoride ($SF_6$). The porphyrin concentration was calculated from the optical "absorbance" at 410 nm and the known extinction coefficient of pyropheophorbide (97 000 $cm^{-1}$ $M^{-1}$). Each data point represents the mean ± standard deviation (SD) for three separate MB preparations. (b) Porshe MB concentration in fetal bovine serum at 37 °C compared with MBs formed without porphyrin−lipid. The optical absorbance at 580 nm due to light scattering is proportional to the MB concentration, as pyropheophorbide does not absorb at this wavelength. Experiments were conducted in triplicate (mean ± SD).

porphyrin components stabilize the shell and further prevent gas dissolution, resulting in a greater yield; however, some regular phospholipid was necessary to maintain the high yield. A 15 mol % porphyrin−lipid formulation encapsulating perfluoropropane gas was chosen for further studies, as these MBs were formed in high yield with a relatively large amount of incorporated porphyrin−lipid.

The properties of porshe MBs were compared to MBs formed in PBS without porphyrin−lipid, using only DSPC and PEG40S. Extensive efforts have been invested in optimizing clinical formulations for improved acoustic MB stability and size distribution using mixtures of phospholipids and additives to the buffer.[16] Although the MBs used here as a control (formed without porphyrin−lipid) were not equivalent to any clinically used agents, a similar simplified formulation has also been used in preclinical studies,[17] and their use in this study served to elucidate precisely the effect of the porphyrin−lipid on the MB shell without the complications of additional factors. To evaluate the influence of the porphyrin−lipid on the MB stability, MBs formed without porphyrin−lipid and porshe MBs were incubated in fetal bovine serum at 37 °C. Optical absorbance due to light scattering was used as a measure of the MB concentration and was monitored over a period of 4 h. Porshe MBs displayed much higher stability than MBs without porphyrin−lipid, remaining nearly twice as long in serum (Figure 2b), further demonstrating that porphyrin−lipid was not only incorporated into the MB shell but also resulted in a more stable MB. This enhanced MB stability may result from the porphyrin-lipid stabilizing the shell and generating an optimal size distribution, which has been shown to be more stable against gas dissolution.[17a,c]

The porshe MBs had a narrow volumetric size distribution that peaked at 2.7 ± 0.2 $\mu$m. MBs smaller than 7 $\mu$m accounted for >95% of the population by volume and >99% by number (Figure S1 in the Supporting Information). Gas volume is often used as a more accurate indicator of US efficacy than number distribution, since larger bubbles dominate the echogenicity of an MB population.[18] Under the same preparation conditions, MBs formed without porphyrin−lipid were more polydisperse (Figure 3a). Monodisperse MBs are of particular interest because

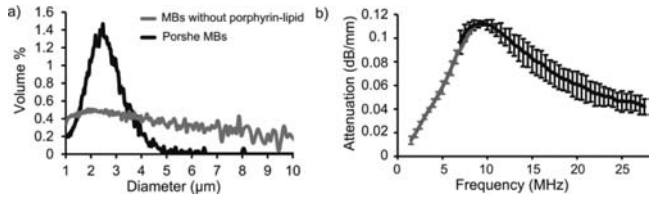


**Figure 3.** Size and acoustic properties of porshe MBs. (a) MBs formed without porphyrin−lipid using mechanical agitation are polydisperse (gray). Porshe MBs have a narrow volumetric distribution (black) with a peak size of 2.7 ± 0.2 $\mu$m (mean ± SD, $n$ = 5). (b) Acoustic attenuation as a function of frequency for porshe MBs: gray, 1.5−8.5 MHz transducer; black, 7−27.5 MHz transducer. For porshe MBs, $f_{res}$ = 9−10 MHz.

of their high acoustic response at the resonant frequency, especially for targeted MBs in molecular imaging, where only a small fraction of the administered dose remains at the target site.[17b] Furthermore, for in vivo imaging, injected doses are required in concentrations of ~$10^9$ MBs/mL. Mechanical agitation is currently the only method that can achieve this level for lipid MB formulations, but the resulting populations are often highly polydisperse. To improve the monodispersity of such MBs thus often requires post synthesis size separation methods (e.g., mechanical filtration or centrifugation), which are not amenable to clinical translation.[17a,19] Porshe MBs intrinsically overcome this limitation. However, to estimate the average porphyrin−lipid content of each MB, porshe MBs were separated from submicrometer particles consisting of residual


dx.doi.org/10.1021/ja305988f | J. Am. Chem. Soc. 2012, 134, 16464−16467

lipids forming vesicles and possible aggregates using a centrifugation method[20] (Figure S2). As the porphyrin−lipid is naturally fluorescent, we determined the porphyrin−lipid concentration in the MB population using fluorescence and UV spectroscopy. A single MB formed from 15% porphyrin−lipid with an average diameter of 1.5 $\mu$m was determined to contain $(1.4 \pm 0.2) \times 10^7$ porphyrins.

The narrow volumetric size distribution of porshe MBs produced a sharp rise in US attenuation with increasing frequency, which exhibited a peak at 9−10 MHz and gradually tapered off by 27.5 MHz (Figure 3b). Attenuation measurements reported for other lipid-encapsulated agents typically showed resonant frequencies below 6 MHz,[18,21] except for Definity,[19] which has an attenuation peak within a similar region as porshe MBs. Thus, having a higher resonance frequency ($f_{res}$) than some commercial lipid-based MBs, porshe MBs may be well-suited for imaging applications exploiting the 5−15 MHz frequency range, including breast imaging, carotid neovascularization, superficial tumors, and endoscopic imaging.

To gain insight into the mechanical properties of porshe MBs, we applied a theoretical approach initially described by de Jong et al.[22] to determine the MB shell stiffness ($S_p$) and shell friction ($S_f$). $S_p$ is a measure of the MB elasticity, while $S_f$ accounts for viscous effects. Briefly, on the basis of a linearized encapsulated microbubble model and the frequency-dependent attenuation and size distribution of the porshe MBs, $S_p$ and $S_f$ were determined using eq 1:

$$f_{res} = \frac{1}{2\pi}\sqrt{\left(\frac{3\gamma p_0}{\rho r^2} + \frac{2S_p}{\rho r^3}\right)\left(1 - \frac{{\delta_r}^2}{2}\right)} \quad (1)$$

where $r$ is the MB radius, $\gamma$ is the polytropic gas index, $p_0$ is the ambient pressure, $\rho$ is the density of the surrounding medium (e.g., water), and $\delta_r$ (proportional to $S_f$) is the total damping. For porshe MBs, $S_p = 5.32 \pm 0.43$ N/m and $S_f = (0.19 \pm 0.14) \times 10^{-6}$ kg/s. Estimates of $S_p$ have been previously reported for several commercial lipid MBs, and the porshe MBs were found to be 3−5 times stiffer than these agents (Table 1). This corresponds to the increase in $f_{res}$ for a given MB size for porshe MBs over lipid MBs. Since the MB stability is related to the properties of the shell and encapsulated gas, it has been suggested by Borden and co-workers[10c,23] that a possible mechanism leading to increased MB stability is an increase in $S_p$ and decreased gas permeability. Increased $S_p$ may result in a greater resistance to collapse. Thus, we hypothesize that the increase in $S_p$ due to the porphyrin−lipid may contribute to the increased yield and serum stability over MBs formed without porphyrin−lipid. However, further investigation is needed to elucidate the influence of the porphyrin−lipid on acoustic dissolution in solution and in vivo. With respect to $S_f$, the determined value of $0.19 \times 10^{-6}$ kg/s between 6 and 13 MHz is at the lower end of the range derived at lower frequencies ($f < 8$ MHz) (Table S1). In comparison with Definity characteristics, porshe MBs are less polydisperse, and Definity contains both smaller and larger MBs, which may potentially possess a larger $S_f$.

**Table 1. Summary of Microbubble Parameters and Shell Properties for Porshe and Commercial Lipid MBs**

| agent | vol. peak size ($\mu$m) | $f_{res}$ (MHz) | $S_p$ (N/m)[a] | $S_f$ ($10^{-6}$ kg/s)[a] |
|---|---|---|---|---|
| Definity[b] | 1−2 and 7[c] | 9−12 | 1.71 ± 0.24 | 0.015 ± 0.015 |
| Sonovue[d] | 5−6 | 1.5−2 | 1.1 | 0.27 |
| Sonazoid[e] | 3.2 ± 0.2 | 3−5 | 1.20 ± 0.07 | 0.48 ± 0.06 |
| **Porshe** | **2.7 ± 0.2** | **9−10** | **5.32 ± 0.43** | **0.19 ± 0.14** |

[a]See Table S1 for the frequency ranges used to estimate the shell parameters. [b]Reference 19. [c]Polydisperse size population with two peaks. [d]Reference 18. [e]References 21 and 22.

Despite having a greater shell stiffness than commercial MBs, porshe MBs maintained the nonlinear properties associated with lipid MBs. Porshe MBs were injected intravenously into mice bearing human breast cancer (MDA-MB-231) xenografts and imaged using a 5 MHz clinical US scanner (Figure 4). The subcutaneous tumor was imaged in B-mode and contrast-mode simultaneously. The B-mode image shows the soft-tissue contrast and outlines a cross section of the entire subcutaneous tumor on the mouse hind leg. The contrast-mode image depicts the nonlinear signal generated solely from porshe MBs. Shortly after injection of porshe MBs, the blood vessels of the tumor became clearly visible, appearing as bright spots that reached maximum signal intensity within 10 s, which allowed the identification of the skin and necrotic core of the tumor. This demonstrates the utility of porshe MBs as a US contrast agent.

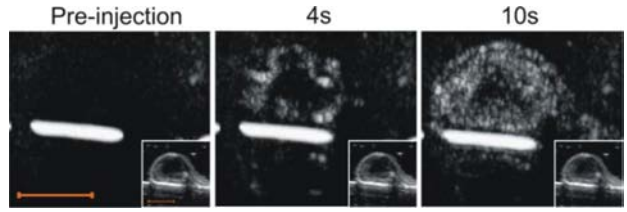


**Figure 4.** In vivo US imaging of porshe MBs in a mouse bearing a MDA-MB-231 xenograft. Contrast-mode images showing the nonlinear contrast from porshe MBs in a cross section of the entire subcutaneous tumor on the mouse hind leg are displayed. The MB signal, shown as bright spots within the tumor after i.v. injection, enabled identification of the tumor vasculature using a 5−12 MHz US transducer. The bright rod-shaped object is an artifact of the system. Insets: B-mode images showing the soft-tissue contrast of the same cross sections as in the contrast-mode images. The B-mode and contrast-mode images were acquired simultaneously. Scale bar: 1 cm.

We previously demonstrated that in a bilayer nanoscale structure, the normally fluorescent porphyrin component of pyropheophorbide−lipid undergoes extreme self-quenching due to the high packing density, making porphysomes a useful PA contrast agent[14a] with a high optical cross section. Similarly, the presence of porphyrin−lipid enables porshe MBs to generate a PA signal that peaks at 700 nm (Figure 5a), corresponding to the Q-band peak in optical absorbance, which is slightly red-shifted from the Q band of pyropheophorbide in solution (Figure S3). This red-shifted peak is further evidence of the porphyrin−porphyrin interactions at the high packing density within the monolayer lipid shell of porshe MBs. MBs formed without porphyrin−lipid, porshe MBs, and MBs without porphyrin−lipid coincubated with equimolar free porphyrin (pyropheophorbide) were photoacoustically imaged in sample wells using a 700 nm, 5 ns pulsed laser and a 10 MHz single-element US transducer (Figure 5b top). The porshe MBs generated a 10-fold greater PA signal than MBs formed without porphyrin−lipid and a 6-fold greater PA signal than MBs without porphyrin−lipid mixed with free porphyrin (Figure S4). This demonstrates not only that the porphyrin must be present in order for the MBs to generate a PA signal but also that the porphyrin must be conjugated to the lipid and present within the MB shell. The organization and high packing density of the porphyrin−lipid conjugates within the MB


dx.doi.org/10.1021/ja305988f | J. Am. Chem. Soc. 2012, 134, 16464−16467

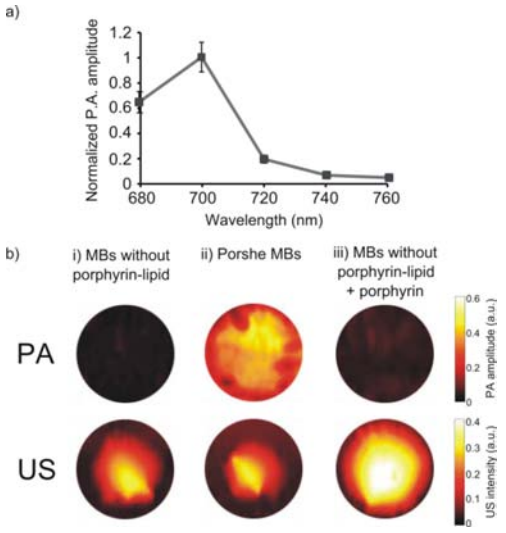


**Figure 5.** PA and US measurements. (a) PA spectrum of porshe MBs (mean ± SD, $n$ = 3). (b) PA (top) and US (bottom) images of MBs formed without porphyrin−lipid, porshe MBs, and MBs without porphyrin−lipid incubated with equimolar pyropheophorbide-$\alpha$ in 9 mm diameter wells within a plastic phantom. PA images were acquired using a 700 nm, 5 ns pulsed laser and a 10 MHz single-element transducer.

shell is required for significant PA signal generation. All of the MB populations generated strong US signals (Figure 5b bottom and Figure S4), confirming that porshe MBs have the capacity to serve as a dual-modality US/PA contrast agent.

In summary, we have developed porshe microbubbles as a dual-modality US/PA contrast agent that shows unexpected physical properties arising from the inclusion of porphyrin−lipid in the shell. These include increased MB yield and increased shell stiffness, resulting in enhanced stability over MBs without porphyrin−lipid. The unique narrow volumetric size distribution of porshe MBs is especially advantageous for molecularly targeted imaging. Porshe MBs possess acoustic properties compatible with clinical and higher-frequency US imaging applications, together with intrinsic PA capabilities. They should have potential both as combined US/PA imaging agents and for emerging MB applications such as drug or gene delivery.

## ■ ASSOCIATED CONTENT

### Ⓢ Supporting Information

Experimental methods and additional data. This material is available free of charge via the Internet at http://pubs.acs.org.

## ■ AUTHOR INFORMATION

### Corresponding Author

gzheng@uhnresearch.ca

### Notes

The authors declare no competing financial interest.

## ■ ACKNOWLEDGMENTS

This work was supported by an International Collaborative R&D Project of the Ministry of Knowledge Economy, South Korea, and also by the Princess Margaret Hospital Foundation, the National Science and Engineering Research Council of Canada, the Canadian Institute for Health Research, the Canadian Foundation of Innovation, and the Joey and Toby Tanenbaum/Brazilian Ball Chair in Prostate Cancer Research.

## ■ REFERENCES

(1) (a) Ferrara, K.; Pollard, R.; Borden, M. *Annu. Rev. Biomed. Eng.* **2007**, *9*, 415. (b) Schutt, E. G.; Klein, D. H.; Mattrey, R. M.; Riess, J. G. *Angew. Chem., Int. Ed.* **2003**, *42*, 3218.

(2) Wilson, S. R.; Burns, P. N. *Radiology* **2010**, *257*, 24.

(3) (a) Dindyal, S.; Kyriakides, C. *Recent Pat. Cardiovasc. Drug Discovery* **2011**, *6*, 27. (b) Moriyasu, F.; Itoh, K. *AJR, Am. J. Roentgenol.* **2009**, *193*, 86.

(4) Kettenbach, J.; Helbich, T. H.; Huber, S.; Zuna, I.; Dock, W. *Eur. J. Radiol.* **2005**, *53*, 238.

(5) Coli, S.; Magnoni, M.; Sangiorgi, G.; Marrocco-Trischitta, M. M.; Melisurgo, G.; Mauriello, A.; Spagnoli, L.; Chiesa, R.; Cianflone, D.; Maseri, A. *J. Am. Coll. Cardiol.* **2008**, *52*, 223.

(6) Lanza, G. M.; Wickline, S. A. *Curr. Probl. Cardiol.* **2003**, *28*, 625.

(7) Hernot, S.; Klibanov, A. L. *Adv. Drug Delivery Rev.* **2008**, *60*, 1153.

(8) Song, J.; Qi, M.; Kaul, S.; Price, R. J. *Circulation* **2002**, *106*, 1550.

(9) Lindner, J. R.; Song, J.; Christiansen, J.; Klibanov, A. L.; Xu, F.; Ley, K. *Circulation* **2001**, *104*, 2107.

(10) (a) Klibanov, A. L.; Hughes, M. S.; Wojdyla, J. K.; Wible, J. H., Jr.; Brandenburger, G. H. *Acad. Radiol.* **2002**, *9* (Suppl. 1), S41. (b) Skyba, D. M.; Price, R. J.; Linka, A. Z.; Skalak, T. C.; Kaul, S. *Circulation* **1998**, *98*, 290. (c) Borden, M. A.; Kruse, D. E.; Caskey, C. F.; Zhao, S.; Dayton, P. A.; Ferrara, K. W. *IEEE Trans. Ultrason. Ferroelectr. Freq. Control* **2005**, *52*, 1992.

(11) (a) Kim, C.; Favazza, C.; Wang, L. V. *Chem Rev* **2010**, *110*, 2756. (b) Jin, Y.; Jia, C.; Huang, S.; O'Donnell, M.; Gao, X. *Na.t Commun.* **2010**, *1*, 41.

(12) (a) Kim, C.; Erpelding, T. N.; Jankovic, L.; Pashley, M. D.; Wang, L. V. *Biomed. Opt. Express* **2010**, *1*, 278. (b) Kolkman, R. G.; Brands, P. J.; Steenbergen, W.; van Leeuwen, T. G. *J. Biomed. Opt.* **2008**, *13*, No. 050510. (c) Niederhauser, J. J.; Jaeger, M.; Lemor, R.; Weber, P.; Frenz, M. *IEEE Trans. Med. Imaging* **2005**, *24*, 436. (d) Needles, A.; Heinmiller, A.; Ephrat, P.; Bilan-Tracey, C.; Trujillo, A.; Theodoropoulos, C.; Hirson, D.; Foster, F. S. *IEEE Ultrason. Symp.* **2010**, 390.

(13) (a) Kim, C.; Qin, R.; Xu, J. S.; Wang, L. V.; Xu, R. *J. Biomed. Opt.* **2010**, *15*, No. 010510. (b) Wilson, K.; Homan, K.; Emelianov, S. *Nat. Commun.* **2012**, *3*, 618. (c) Strohm, E.; Rui, M.; Gorelikov, I.; Matsuura, N.; Kolios, M. *Biomed. Opt. Express* **2011**, *2*, 1432. (d) Wang, Y.; Liao, A.; Chen, J.; Lee, Y.; Wang, C.; Li, P. *Proc. SPIE* **2011**, *7899*, No. 78993V.

(14) (a) Lovell, J. F.; Jin, C. S.; Huynh, E.; Jin, H.; Kim, C.; Rubinstein, J. L.; Chan, W. C.; Cao, W.; Wang, L. V.; Zheng, G. *Nat. Mater.* **2011**, *10*, 324. (b) Lovell, J. F.; Jin, C. S.; Huynh, E.; Macdonald, T. D.; Cao, W.; Zheng, G. *Angew. Chem., Int. Ed.* **2012**, *51*, 2429.

(15) Klibanov, A. L. *Med. Biol. Eng. Comput.* **2009**, *47*, 875.

(16) Unger, E. C.; Porter, T.; Culp, W.; Labell, R.; Matsunaga, T.; Zutshi, R. *Adv. Drug Delivery Rev.* **2004**, *56*, 1291.

(17) (a) Feshitan, J. A.; Chen, C. C.; Kwan, J. J.; Borden, M. A. *J. Colloid Interface Sci.* **2009**, *329*, 316. (b) Streeter, J. E.; Gessner, R.; Miles, I.; Dayton, P. A. *Mol. Imaging* **2010**, *9*, 87. (c) Talu, E.; Hettiarachchi, K.; Powell, R. L.; Lee, A. P.; Dayton, P. A.; Longo, M. L. *Langmuir* **2008**, *24*, 1745.

(18) Gorce, J. M.; Arditi, M.; Schneider, M. *Invest. Radiol.* **2000**, *35*, 661.

(19) Goertz, D. E.; de Jong, N.; van der Steen, A. F. *Ultrasound Med. Biol.* **2007**, *33*, 1376.

(20) Wheatley, M. A.; Forsberg, F.; Dube, N.; Patel, M.; Oeffinger, B. E. *Ultrasound Med. Biol.* **2006**, *32*, 83.

(21) (a) Sarkar, K.; Shi, W. T.; Chatterjee, D.; Forsberg, F. *J. Acoust. Soc. Am.* **2005**, *118*, 539. (b) Sontum, P. C.; Ostensen, J.; Dyrstad, K.; Hoff, L. *Invest. Radiol.* **1999**, *34*, 268.

(22) de Jong, N.; Hoff, L.; Skotland, T.; Bom, N. *Ultrasonics* **1992**, *30*, 95.

(23) Borden, M. A.; Longo, M. L. *Langmuir* **2002**, *18*, 9225.